Electrochemical doping during light emission in polymer light-emitting electrochemical cells

Nathaniel D. Robinson,[1,*] Junfeng Fang,[2] Piotr Matyba,[2] and Ludvig Edman[2,†]
[1]*The Separations and Transport Group, Department of Physics, Chemistry and Biology, Linköping University, SE 581-83 Linköping, Sweden*
[2]*The Organic Photonics and Electronics Group, Department of Physics, Umeå University, SE 901-87 Umeå, Sweden*
(Received 8 August 2008; published 1 December 2008)

Polymer light-emitting electrochemical cells (LECs), the electrochemical analog of light-emitting diodes, are relatively simple to manufacture yet difficult to understand. The combination of ionic and electronic charge carriers make for a richly complex electrochemical device. This paper addresses two curious observations from wide-gap planar LEC experiments: (1) Both the current and light intensity continue to increase with time long after the *p-n* junction has formed. (2) The light-emitting *p-n* junction often moves, both "straightening out" and migrating toward the cathode, with time. We propose that these phenomena are explained by the continuation of electrochemical doping even after the *p-n* junction has formed. We hope that this understanding will help to solve issues such as the limited lifetime of LECs and will help to make them a more practical device in commercial and scientific applications.

DOI: 10.1103/PhysRevB.78.245202 PACS number(s): 82.47.Tp, 72.20.−i

I. INTRODUCTION

Light-emitting devices based on organic electronic materials are heralded as an inexpensive and efficient alternative to traditional incandescent and fluorescent lamps as well as informational displays [e.g., liquid crystal display (LCD) screens]. The majority of research and commercial development in this area is based on organic light-emitting diodes (OLEDs). Light-emitting electrochemical cells (LECs) have a structure similar to OLEDs but include mobile ions in the active layer, causing them to exhibit very different operational characteristics. LECs will likely be simpler and cheaper to manufacture than OLEDs since they are insensitive to the thickness of the active layers, so that, e.g., roll-to-roll manufacturing should be possible. Similarly, LECs do not require a large difference in electrode work function to operate, meaning that highly reactive metals such as Ca are not necessary. Today's state-of-the-art LECs are currently plagued by relatively short lifetimes and, more importantly, are poorly understood. There are widely varying pictures of how the devices operate competing for acceptance.

We and others have described the operation of wide-gap planar LECs, taking advantage of the insensitivity of the device's performance on the interelectrode distance.[1,2] Wide-gap LECs are admittedly more useful for studying the mechanisms of device operation than for practical applications; however, they allow us to peer directly into the interelectrode gap and observe the physical processes at hand, which is something that cannot be done in sandwich-shaped LECs and OLEDs. Directly observing the internal operation of LECs elucidates mechanisms which govern their behavior[3] and has led us to favor, for example, the electrochemical doping-based model proposed by Pei *et al.*[1,4] over the diffusion-based model proposed by deMello *et al.*[5] However, this opinion is far from unanimous in the scientific community, fostering a rather lively debate.[6] For the sake of brevity, we will continue the discussion in this paper from the perspective of the electrochemical doping model of LEC operation.

The sequence of events that occur after a potential has been applied to an LEC according to the electrochemical doping model can be summarized as follows: (1) Electrochemical doping of the conjugated polymer in the active material causes *p*- and *n*-doped regions to grow from the metallic anode and cathode, respectively. (2) These regions grow until they collide, forming a *p-n* junction. (3) Further electrons and holes transported to the *p-n* junction recombine, decaying both thermally and emissively. This paper closely examines these processes and hypothesizes, based on experimental observations, that the doping process described in steps (1) and (2) does not dope the polymer to the extent available given the potential applied to the device,[7] but that further doping of the partially doped polymer takes place *after* the *p-n* junction has formed. The expected and observed consequences are that the current and the light emitted by the device increase with time *after* the *p-n* junction formation and that the *p-n* junction can move and straighten out with time.

II. EXPERIMENT

A. LEC preparation

The conjugated polymer poly[2-methoxy-5-(2-ethylhexyloxy)-1,4-phenylenevinylene (PPV)] (MEH-PPV) (Organic Vision) was used as received. Poly(ethylene oxide) (PEO) ($M_w = 5 \times 10^6$, Aldrich) and the salt KCF_3SO_3 (98%, Alfa Aesar) were dried at a temperature (T) of 323 and 473 K, respectively, under vacuum. Master solutions of 10 mg/mL concentration were prepared. MEH-PPV was dissolved in chloroform (>99%, anhydrous, Aldrich) and PEO and KCF_3SO_3 were dissolved separately in cyclohexanone (99%, Merck). A blend solution was prepared by mixing the master solutions together in a mass ratio of MEH-PPV:PEO:KCF_3SO_3=1:1.35:0.25, followed by stirring on a magnetic hot plate at T=323 K for at least 5 h.

The 1.5×1.5 cm^2 glass substrates were cleaned by subsequent ultrasonic treatment in detergent, acetone, and iso-

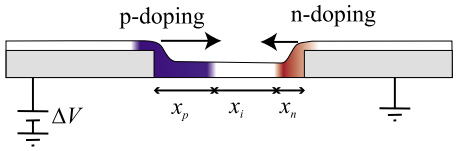

FIG. 1. (Color online) Side view of a planar wide-gap LEC device, showing the anode (left) and cathode (right) connected with a conjugated polymer/electrolyte blend film. The *p*- and *n*-doped regions are shown growing from the anodic and cathodic Au electrodes, respectively.

propanol solutions. The 100-nm-thick Au electrodes were deposited onto the cleaned glass substrates by thermal evaporation at $p<2\times10^{-4}$ Pa. The interelectrode gap was established by an Al shadow mask.

The blend solution was deposited onto the Au electrodes by spin coating at 800 rpm for 60 s, which resulted in active material films with a thickness of 150 nm. The films were thereafter dried on a hot plate at $T=333$ K for at least 5 h. Finally, immediately preceding a measurement, *in situ* drying in a cryostat for 2 h at $T=360$ K and under vacuum ($p<10^{-3}$ Pa) took place. All of the above device preparation procedures, with the exception of cleaning of substrates were carried out in N_2-filled glove boxes ($O_2<3$ ppm and $H_2O<0.5$ ppm).

The characterization of devices was performed under vacuum ($p<10^{-3}$ Pa) at $T=360$ K in an optical-access cryostat. The elevated temperature allows for a significant ionic conductivity in the active material, which in turn results in a low turn-on voltage and reasonably short turn-on time.[8] A computer-controlled source-measure unit (Keithley 2400) was employed to apply voltage and to measure the resulting current. The photographs of the doping progression were recorded through the optical window of the cryostat, using a digital camera (Canon EOS 20D) equipped with a macro lens, and under UV ($\lambda=365$ nm) illumination.

B. Image analysis

Images were analyzed by hand with the assistance of ORIGIN software (Origin Laboratories). The location of each electrode and the *p*-doping front was measured in each original digital image. The *p*-doping-front location was converted to physical units based on the known interelectrode gap width.

III. RESULTS

In a previous paper,[9] we demonstrated that the doping-front progression observed during turn on in LECs is limited by the transport of ions between the doping fronts, where neutral polymer is oxidized and reduced to *p*-doped and *n*-doped polymers, respectively. A sketch of this process occurring in a planar device with Au electrodes covered by a mixture of a conjugated polymer and electrolyte is shown in Fig. 1. Photographs of this process, including the formation of a *p*-*n* junction and the subsequent light emission, are shown in Fig. 2.

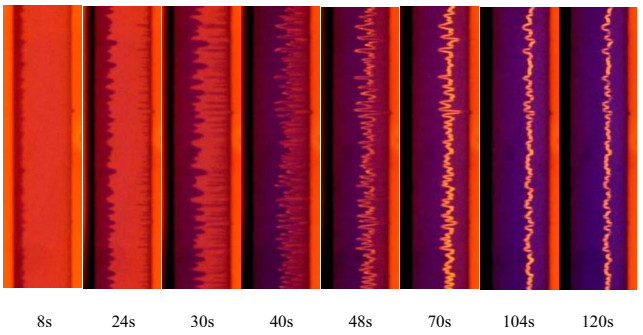

FIG. 2. (Color online) Photographs of (UV-light-initiated) photoluminescence and electroluminescence from a 1 mm planar MEH-PPV LEC during turn on and operation. The anodic metal electrode is on the left and cathodic on the right. The device was operated at 10 V. The time each image was taken (relative to the application of the 10 V potential) appears under each image.

The half reactions involved in the doping process at the anode and cathode are, respectively,

$$p^0 + h^+ + X^- \rightarrow p^+X^-, \tag{1}$$

$$p^0 + e^- + M^+ \rightarrow M^+p^-, \tag{2}$$

where p^0 represents an undoped polymer segment, h^+ represents a hole, e^- represents an electron, M^+X^- represents the salt found in the electrolyte, and p^+ and p^- represent *p*-doped and *n*-doped polymer segments, respectively.

The model we presented in Ref. 9 requires that the electronic current consumed by the device be proportional to the rate of doping-front propagation during device turn on; in other words that the doping-front progression produces a constant doping concentration behind the front. A comparison between the *p*-doping-front position and integrated current (charge) versus time is shown in Fig. 3. The correspondence between the optical and electronic observation is strong; the charge consumed can be predicted by multiplying

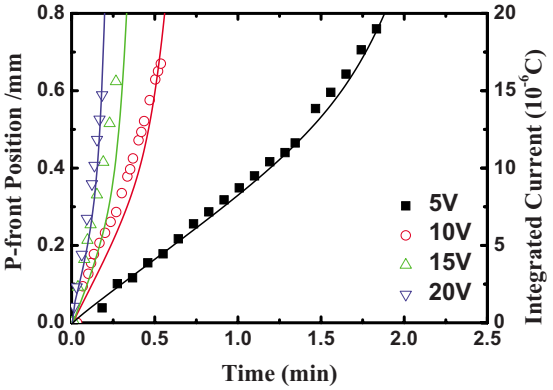

FIG. 3. (Color online) *p*-doping-front position (symbols and left-hand axis) and accumulated charge (lines and right-hand axis) during the turn-on process for 1 mm planar LECs operated at the potentials indicated in the legend. The accumulated charge was calculated by integrating the current driven through the device. The results are the averages calculated from at least five independent measurements on pristine devices.

the front position by a constant, which includes the thickness and width of the film and the average doping concentration value during front progression. This factor does not vary, even when the applied potential varies between 5 and 20 V,[10–12] thus confirming our previous assumption that the doping front progressing indeed takes place at a constant doping concentration. The relatively small size of the *n*-doped region and side reactions that compete with the initiation of the *n*-doping process[12] prevents the analogous analysis of the *n*-doping front.

Our herein proposed view of the evolution of the applied potential profile within an LEC during device turn on is shown as a series of sketches in Fig. 4. Charge-carrier (ion, hole, and electron) motion is also included. The potential applied between the electrodes is approximately twice the band gap of the conjugated polymer. The potential drop in the Au electrodes is negligible compared to that in the devices, and the contacts between *p*- and *n*-doped polymers and the Au electrodes are Ohmic.

Figure 4(a) illustrates a point in time where the *p*- and *n*-type doping fronts are progressing toward one another but are still far apart. The band-gap potential drops over the two interfaces between the *p*- and *n*-doped polymers and the undoped region, while the majority of the remaining potential (the overpotential) drops over the undoped polymer region between the *p*- and *n*-doping fronts where charge is transported by bulky ions. At the interfaces between undoped and doped polymers, a large concentration of ions (effectively the ionic portion of an electric double layer) aids charge injection, converting the undoped polymer and advancing the doping front in the process. Compared to the undoped region, the *p*- and *n*-doped polymer regions exhibit low resistance at this stage, which results in a small potential drop in these regions. This also means that there is relatively little ion motion in the doped regions compared to the undoped region.

As the doping fronts approach each other and the width of the undoped region diminishes, the resistance of the undoped polymer region decreases while the resistance of the doped regions increases. The point at which the potential drop in the *p*- and *n*-doped regions becomes as large as the drop over the undoped region can be estimated based on the relative conductivities of the two regions. The measured ionic conductivity (σ_i) for the active material is on the order of 10^{-4} S cm^{-1}.[4,8] The electronic conductivity of *doped* PPVs (σ_{doped}) can be as high as ~ 1 S cm^{-1},[4,11–13] but the MEH-PPV material used here is amorphous, blended with an electrolyte, and not fully doped during doping-front progression and accordingly far from optimized from a conductivity perspective; thus, it is reasonable to expect that σ_{doped} during doping-front progression is of the order of 10^{-2} S cm^{-1}. The point at which the potential drop in the doped regions is the same as the drop over the undoped region can be estimated as follows:

$$V_i \sim V_{\text{doped}}, \tag{3}$$

$$\frac{x_i}{\sigma_i} \sim \frac{x_{\text{doped}}}{\sigma_{\text{doped}}}, \tag{4}$$

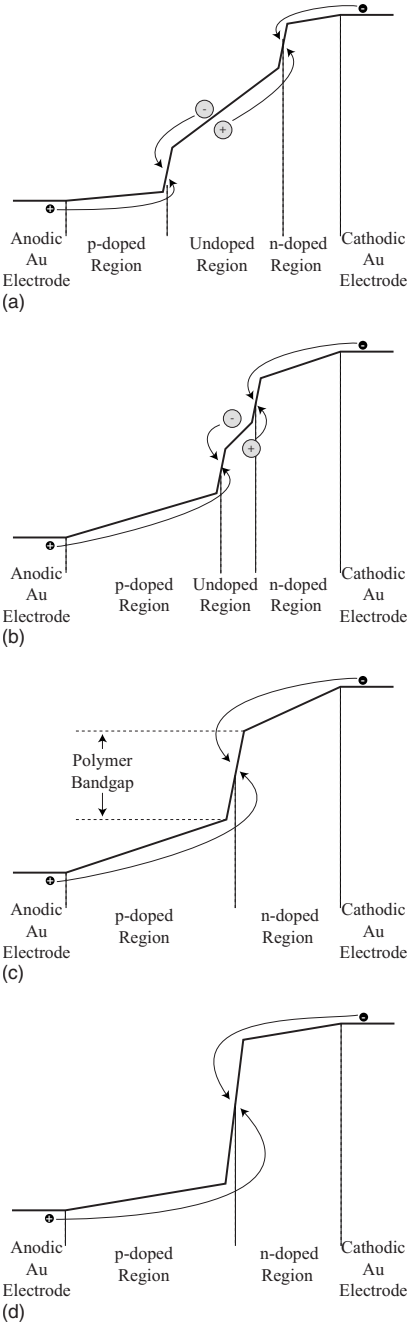

FIG. 4. Qualitative evolution of the applied potential and charge-carrier motion in a wide-gap LEC with an applied potential approximately twice the polymer's band gap; in other words, the overpotential and the band-gap potential are approximately the same. (a) Early in the process, the overpotential drops primarily over the undoped region where ion motion limits the current. (b) As the width of the undoped region diminishes, the overpotential drop in each doped polymer region becomes significant and the device is no longer ion limited. (c) When the *p*- and *n*-doped regions meet, a *p*-*n* junction is formed and the device begins to emit (weak) light. At this point, the potential drop over the *p*-*n* junction is approximately the polymer band gap, while the remaining potential (i.e., the overpotential) drops over the doped regions. (d) Further doping within the *p*- and *n*-doped regions decreases their resistance, leaving the *p*-*n* junction as the major resistance in the device over which essentially all the applied potential drops.

$$x_i \sim (1 - x_i)\frac{\sigma_i}{\sigma_{\text{doped}}}, \tag{5}$$

$$x_i \sim \left(1 + \frac{\sigma_{\text{doped}}}{\sigma_i}\right)^{-1}, \tag{6}$$

keeping in mind that the current density $j = V\sigma/x$ is uniform across the device and $x_i + x_{\text{doped}} = 1$. Using the values above for σ_i and σ_{doped}, one can calculate $x_i \sim 10^{-2}$ or an undoped region width of about 10 μm for the 1-mm-wide interelectrode gap in the devices studied here. The applied potential profile within the device at this point in time is captured by the sketch in Fig. 4(b).

Figure 4(c) shows the applied potential profile at the point when the *p-n* junction first forms. The initial potential drop over the *p-n* junction is only slightly larger than the polymer's band gap. The rest of the potential drops resistively over the *p*- and *n*-doped regions. Most of the holes and electrons that travel to the *p-n* junction meet there and recombine, often causing light emission, but this electronic current is relatively small due to the relatively high electronic resistance in the doped regions.

A consequence of the hypothesis of this paper is facilitated by a comparison between Figs. 4(c) and 4(d). Directly after the *p-n* junction formation, the rather large potential drop within the *p*- and *n*-doped regions [see Fig. 4(c)] will cause migration of free ions (in addition to the migration of electrons) within the doped regions. The ratio of ionic to electronic migratory motion can be estimated from the $\sigma_i/\sigma_{\text{doped}}$ conductivity ratio.[14] When a migrating ion meets a migrating electron within the doped region, further doping can take place. The consequential decrease in the electronic resistance of the doped regions will eventually cause nearly the entire potential to drop over the *p-n* junction [see Fig. 4(d)]. It is important to understand that this scenario is based on the assumption that the conjugated polymer is not fully doped when the doping fronts advance forward, and that further doping accordingly can take place after the initial *p-n* junction has formed. Below, we present evidence that strongly supports this hypothesis.

The hypothesis that the *p*- and *n*-doped regions are only partially doped when the *p-n* junction is formed comes from observations of the current passing through the device and the light emitted by it. Both increase dramatically for several seconds after *p-n* junction formation. The change in light emission can be seen in the photographs shown in Fig. 2. The *p-n* junction has started to form in many locations already 40 s after the 10 V potential was applied. By 48 s, it is clearly complete. However, the brightness continues to increase, as clearly visible in the image taken at 70 s. Near this point, the brightness, followed by the current, begins to decrease as the device begins to "burn out." See Wågberg *et al.*[15] for a discussion of this process. The intensity of light emission versus time recorded by a photodiode connected to a device similar to that shown in Fig. 2 is presented in Fig. 5, showing quantitatively the same result visible in the photographs.

The evolution of the current density with time at various drive voltages is presented in Fig. 6. The times for continuous *p-n* junction formation are indicated by the arrows. It is clear that the current increased significantly after the initial formation of the *p-n* junction. Comparing the current data for the 10 V devices in Fig. 6 to the light-emission data in Fig. 5, it is clear that the increase in each is correlated. However, the current does not decrease as quickly as the light emission does when burnout occurs (after ~80 s).

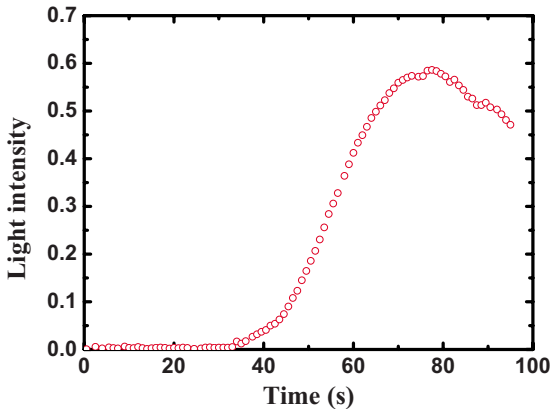

FIG. 5. (Color online) Light emission versus time for an LEC operated at 10 V. The continuous *p-n* junction was formed at ~35 s in this specific device.

Besides the increase in current and light emission, there are additional consequences of electrochemical doping after the formation of the *p-n* junction. For example, the *p-n* junction often appears to move and "straighten out" with time, as can be seen by comparing the images captured at 48, 70, and 104 s in Fig. 2. At 48 s, the *p-n* junction has just formed at a location determined by the relative doping concentrations resulting from the turn-on process (see Robinson *et al.*[9]). However, this is clearly not the final shape and location of the *p-n* junction.

As discussed above, additional doping is commonly observed in LEC devices after the initial *p-n* junction formation. This additional doping can progress via two routes. The first is symmetric and simply involves further *p* doping in the

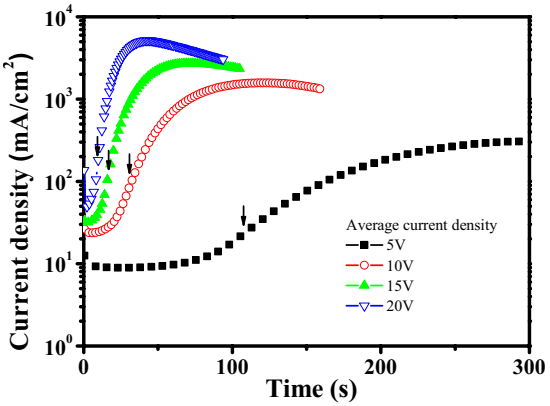

FIG. 6. (Color online) Current density through LEC devices versus time. The devices were operated at the potentials indicated in the legend. The average time at which a continuous *p-n* junction formed for each data set is indicated by a vertical arrow. The data are the average of ≥5 measurements at each applied potential.

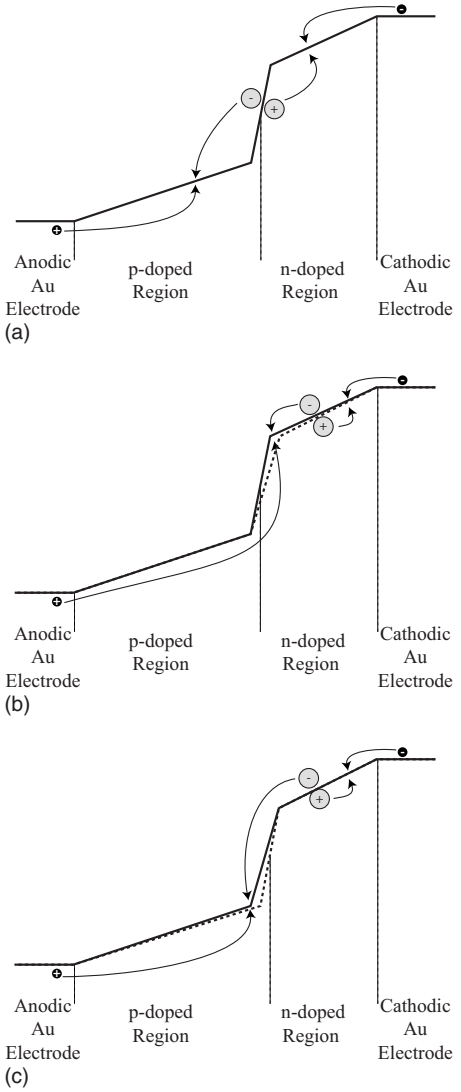

FIG. 7. Charge-carrier transport in electrochemical doping processes after the *p-n* junction formation. (a) Both *p*- and *n*-type doping occur throughout the regions that were partially doped during the turn-on process, decreasing the resistance of both regions. (b) The *n*-doped polymer adjacent to the *p-n* junction is undoped, decreasing the size of the *n*-doped region (the first step in the second route is described in the text). This widens the *p-n* junction as indicated qualitatively by the dashed line. (c) The *p*-doped region expands by doping undoped polymer at the near edge of the *p-n* junction, completing the "step" of the *p-n* junction toward the cathode.

p-doped region and *n* doping in the *n*-doped region, decreasing the resistance of each side. The ion and electron or hole transport required for the reaction is shown in Fig. 7(a). This is similar to the mechanism that initially doped the device during turn on [Fig. 4(a)], except that doping takes place within each doped region where it was (primarily) confined to the doped/undoped polymer interface during device turn on. This route will lead to an increase in both current and brightness from a stationary *p-n* junction.

The second route, on the other hand, causes the *p-n* junction to move, as one doped region is consumed and the other doped region expands. For brevity, we will describe the consumption of the *n*-doped polymer and expansion of the *p*-doped polymer region. However, the reverse process can also occur, depending on, e.g., the relative potential profiles and position where the *p-n* junction initially formed.

The second route requires two steps, which likely occur simultaneously. The first involves the undoping (oxidation) of the *n*-doped (reduced) polymer,

$$M^+p^- + h^+ \rightarrow p^0 + M^+ \tag{7}$$

and further *n* doping within the *n*-doped polymer region according to Eq. (2). This reaction causes a net decrease in doping at the *n*-doped/undoped polymer interface, effectively establishing a widened undoped region at the cathodic side of the *p-n* junction. The ion and hole or electron transport involved in this step is illustrated in Fig. 7(b). The second step *p* dopes a neutral polymer segment at the *p*-doped/undoped polymer interface (the anodic side of the *p-n* junction) via Eq. (1) and further *n* dopes the polymer in the *n*-doped region via Eq. (2), as illustrated in Fig. 7(c). The net result of the overall reaction is

$$2p^0 + M^+X^- + e^- + h^+ \rightarrow p^+X^- + M^+p^-. \tag{8}$$

Notice that this reaction is exactly the sum of Eqs. (1) and (2), the process that caused the *p*- and *n*-doped regions to grow until they met. However, the physical result is now the net motion of the *p-n* junction toward the cathode and an increase in doping concentration in the *n*-doped region. As stated previously, the analogous reaction driving the *p-n* junction toward the anode and increasing the doping concentration in the *p*-doped region is also possible.

The motion of the *p-n* junction is visible in the photographs in Fig. 2, for example, between 48 and 70 s and again between 70 and 104 s, where the interface between the *p*- and *n*-doped sides has become shorter (the *p-n* junction has straightened out). In addition to decreasing its length, the *p-n* junction also tends to move toward the cathode with time. This motion has been observed by others as well, including Gao and Dane[16] who described it as a "charge compensation process." We see it as an evolution from the initial position established during the turn-on process toward one in which the free energy of the system is minimized.

Detailed understanding of why the doping reactions stop at a certain doping fraction during the front progression (see Fig. 3 and related text and Refs. 10–12) is currently lacking. However, we note that other conjugated polymers such as poly(3-hexylthiophene) (P3HT) demonstrate a clear highly nonlinear increase in hole mobility at doping fractions starting around 1%, while they can be doped to about 20%.[17] Direct measurements of the transport of holes in PPV (undecorated backbone of the MEH-PPV used in the devices we have studied) show a 5 decade change in mobility between doping fractions of 0 and 20%.[18] A similar onset in the mobility with concentration can be expected from the MEH-PPV used in the LECs reported here. Considering that the apparently generic doping fraction for doping-front progression in LECs is ~10%,[19] it is tempting to correlate the doping fraction for front progression with the sharp nonlinear increase in mobility. It is notable that this threshold doping value does not correspond to the maximum doping value,

and that the electronic conductivity (the product of mobility and concentration) will be accordingly larger at higher doping fractions. We also note that Johansson *et al.*[20] reported that a *p*-doping front in a P3HT film advanced before doping was complete, as demonstrated by the small electrochemical current that continued after the doping front had consumed the entire polymer film in their experiment.

It is clear that the vast complexity of LEC operation, encompassing mixed electronic and ionic transport in parallel with electrochemical doping reactions, requires a full modeling study including recent experimental findings in order to shed light on the details of the various processes. Nevertheless, we find it striking that the simple qualitative operational model outlined herein is capable of rationalizing several experimental observations that up to now have been somewhat of an enigma.

At this stage, it is relevant to present a word of caution. It should be noted that the scenario described above where a wide-gap LEC shifts from being solely ion-transport limited to become influenced by electron-transport effects is probably not relevant for much thinner sandwich-type devices in which a 100 nm polymer blend fills the gap between parallel metal and transparent electrodes. In this case, the model would predict that the potential drop in the doped regions would match that in the undoped region when the undoped region is ~ 1 nm wide, which in all likelihood is smaller than the width of the *p-n* junction. Thus, the turn-on process will differ between planar wide-gap LECs and sandwich-type devices and the lessons learned from experiments and analyses such as the one presented here should be applied with caution to devices with significantly smaller interelectrode dimension.

Finally, it should also be noted that the internal potential profiles presented in this paper differ from those measured experimentally in analogous devices using scanning Kelvin probe microscopy.[21] We suspect that the devices measured by Pingree *et al.*[21] lacked significant *n*-type doping during the turn-on process (presumably due to electrochemical and/or chemical side reactions),[11,12] placing the *p-n* junction very near the cathodic metal electrode. Ensuring that both *p*- and *n*-type doping occurs so that the *p-n* junction forms a visible distance from each metal electrode is a requirement if one is to observe all of the elements of the potential profile sketched in Fig. 4 of this paper.

IV. CONCLUSION

In summary, based on experimental observations and the simple descriptive model presented in this work, we conclude that doping in planar LECs must continue to occur even after the initial doping front has passed. This process continues even after electroluminescence is observed and is probably the mechanism by which the emission zone (*p-n* junction) moves with time and both the current and light intensity continue to increase long after the *p-n* junction has formed. We hope that this understanding will help to solve issues such as the limited lifetime of LECs and will help to make them a more practical device in commercial and scientific applications.

ACKNOWLEDGMENTS

N.D.R. would like to thank the Swedish Research Council (Vetenskapsrådet) and Norrköpings Kommun (Forskning och Framtid) for financial support. The authors from Umeå are grateful to Vetenskapsrådet, Kungliga Vetenskapsakademin, and Stiftelsen J. Gust. Richert for generous financial support.

*natro@ifm.liu.se
†ludvig.edman@physics.umu.se

[1] Q. B. Pei, G. Yu, C. Zhang, Y. Yang, and A. J. Heeger, Science **269**, 1086 (1995).
[2] L. Edman, M. Pauchard, D. Moses, and A. J. Heeger, J. Appl. Phys. **95**, 4357 (2004); S. Alem and J. Gao, Org. Electron. **9**, 347 (2008); J. M. Leger, S. A. Carter, and B. Ruhstaller, J. Appl. Phys. **98**, 124907 (2005); G. Mauthner, K. Landfester, A. Köck, H. Brückl, M. Kast, C. Stepper, and E. J. W. List, Org. Electron. **9**, 164 (2008); J. D. Slinker, J. A. DeFranco, M. J. Jaquith, W. R. Silveira, Y.-W. Zhong, J. M. Moran-Mirabal, H. G. Craighead, H. D. Abruña, J. A. Marohn, and G. G. Malliaras, Nature Mater. **6**, 894 (2007); J. Morgado, R. H. Friend, F. Cacialli, B. S. Chuah, S. C. Moratti, and A. B. Holmes, J. Appl. Phys. **86**, 6392 (1999).
[3] J. Gao and J. Dane, Appl. Phys. Lett. **83**, 3027 (2003).
[4] Q. Pei, Y. Yang, G. Yu, C. Zhang, and A. J. Heeger, J. Am. Chem. Soc. **118**, 3922 (1996).
[5] J. C. deMello, N. Tessler, S. C. Graham, and R. H. Friend, Phys. Rev. B **57**, 12951 (1998); J. C. deMello, *ibid.* **66**, 235210 (2002).
[6] G. G. Malliaras, J. D. Slinker, J. A. DeFranco, M. J. Jaquith, W. R. Silveira, Y.-W. Zhong, J. M. Moran-Mirabal, H. G. Craighead, H. D. Abruña, and J. A. Marohn, Nature Mater. **7**, 168 (2008); Q. Pei and A. J. Heeger, *ibid.* **7**, 167 (2008).
[7] For example, applying 5V between MEH-PPV coated electrodes in a liquid electrolyte during cyclic voltammetry is more than enough to "fully dope" the polymer. Note, however, that the herein investigated LEC devices are ion-transport limited during the initial operation when the doping fronts traverse the interelectrode gap, and that only a limited amount of the applied potential (approximately the band-gap potential) accordingly is available for the doping process.
[8] J.-H. Shin, A. Dzwilewski, A. Iwasiewicz, S. Xiao, Å. Fransson, G. N. Ankah, and L. Edman, Appl. Phys. Lett. **89**, 013509 (2006).
[9] N. D. Robinson, J.-H. Shin, M. Berggren, and L. Edman, Phys. Rev. B **74**, 155210 (2006).
[10] J.-H. Shin, N. D. Robinson, S. Xiao, and L. Edman, Adv. Funct. Mater. **17**, 1807 (2007).
[11] J. Fang, Y. Yang, and L. Edman, Appl. Phys. Lett. **93**, 063503 (2008).
[12] J. Fang, P. Matyba, N. D. Robinson, and L. Edman, J. Am. Chem. Soc. **130**, 4562 (2008).

[13] H. C. F. Martens, I. N. Hulea, I. Romijn, H. B. Brom, W. F. Pasveer, and M. A. J. Michels, Phys. Rev. B **67**, 121203(R) (2003).
[14] In the devices shown here, there is a rather large excess of ions available, so that the ionic conductivity of the blend will not change dramatically as they are consumed in the doping process.
[15] T. Wågberg, P. R. Hania, N. D. Robinson, J.-H. Shin, P. Matyba, and L. Edman, Adv. Mater. (Weinheim, Ger.) **20**, 1744 (2008).
[16] J. Gao and J. Dane, Appl. Phys. Lett. **84**, 2778 (2004).
[17] X. Jiang, Y. Harima, K. Yamashita, Y. Tada, J. Ohshita, and A. Kunai, Chem. Phys. Lett. **364**, 616 (2002).
[18] I. N. Hulea, H. B. Brom, A. J. Houtepen, D. Vanmaekelbergh, J. J. Kelly, and E. A. Meulenkamp, Phys. Rev. Lett. **93**, 166601 (2004).
[19] P. Matyba, M. R. Andersson, and L. Edman, Org. Electron. **9**, 699 (2008).
[20] T. Johansson, N.-K. Persson, and O. Inganäs, J. Electrochem. Soc. **151**, E119 (2004).
[21] L. S. C. Pingree, D. B. Rodovsky, D. C. Coffey, G. P. Bartholomew, and D. S. Ginger, J. Am. Chem. Soc. **129**, 15903 (2007).